

# PREPARATION OF GOLD NANOPARTICLES FUNCTIONALIZED WITH FOLIC ACID FOR TARGETED DRUG DELIVERY IN OVARIAN CANCER CELLS

Fatima Batool<sup>1</sup>, Adnan<sup>2</sup>, Waqar Ahmad<sup>3</sup>

<sup>1</sup>Department of Biotechnology, COMSATS University Islamabad, Abbottabad Campus, Pakistan

<sup>2</sup>Department of Chemical Engineering, Pakistan Institute of Engineering and Technology (PIEAS) Pakistan

<sup>4</sup>Department of Chemistry, The University of Lahore, Sargodha Campus, Punjab, Pakistan

<sup>1</sup>fatimahyousafzai@gmail.com, <sup>2</sup>enr.adnanaliawan@gmail.com, <sup>3</sup>chemistwaqar123@gmail.com

DOI: <https://doi.org/10.5281/zenodo.17597062>

## Keywords

gold nanoparticles; folic acid; ovarian cancer; targeted delivery; doxorubicin; folate receptor

## Article History

Received: 20 September 2025

Accepted: 30 October 2025

Published: 13 November 2025

Copyright @Author

Corresponding Author: \*  
Fatima Batool

## Abstract

Targeted drug delivery systems have emerged as powerful strategies for improving the therapeutic index of chemotherapeutic agents while reducing systemic toxicity. In this study, folic acid-functionalized gold nanoparticles (FA-AuNPs) were developed as a targeted delivery vehicle for folate receptor-positive ovarian cancer cells (SKOV-3). Gold nanoparticles were synthesized via the Turkevich citrate reduction method, producing stable, monodisperse, spherical nanoparticles with an average diameter of  $20 \pm 2$  nm. Functionalization with folic acid (FA) was achieved through EDC/NHS-mediated carbodiimide coupling, enabling specific targeting of cancer cells overexpressing folate receptors. UV-Vis spectroscopy revealed a characteristic plasmon resonance peak at **530 nm**, confirming AuNP formation, while Transmission Electron Microscopy (TEM) confirmed uniform morphology. FTIR spectra showed absorption bands corresponding to C=O and N-H stretching, validating folate conjugation to the nanoparticle surface. The anticancer drug doxorubicin (DOX) was loaded onto FA-AuNPs with an  **$85 \pm 3\%$  loading efficiency**, followed by sustained release over 48 hours in physiological media. Cellular uptake studies in SKOV-3 ovarian cancer cells demonstrated a **3.7-fold** increase in internalization of FA-AuNPs compared to non-functionalized AuNPs. Furthermore, MTT assays revealed significantly enhanced cytotoxicity toward cancer cells with minimal toxicity to normal fibroblasts. These results confirm that FA-functionalized AuNPs provide a biocompatible, stable, and receptor-specific nanocarrier system capable of enhancing targeted drug delivery and minimizing off-target side effects, offering substantial promise for the selective treatment of ovarian cancer.

## INTRODUCTION

Cancer remains one of the most devastating global health challenges, characterized by uncontrolled cell proliferation, metastasis, and resistance to conventional therapies. Among gynecological malignancies, ovarian cancer ranks as the most lethal, often diagnosed at advanced stages due to asymptomatic progression and lack of effective screening tools (Siegel et al., 2023). Conventional

chemotherapy with agents such as doxorubicin and cisplatin is associated with severe systemic toxicity, rapid clearance, and limited tumor selectivity (Ghosh et al., 2020). Consequently, there has been increasing emphasis on developing nanotechnology-based targeted delivery systems that enhance drug accumulation in tumor tissues while minimizing adverse effects on healthy cells.

Gold nanoparticles (AuNPs) have emerged as one of the most promising nanocarriers for cancer therapy due to their biocompatibility, chemical inertness, tunable size, and ease of surface modification (Dykman & Khlebtsov, 2018). Their strong surface plasmon resonance (SPR) also enables real-time tracking and photothermal applications, adding multifunctionality to drug delivery systems. AuNPs possess large surface areas suitable for conjugating ligands, polymers, and therapeutic molecules through covalent or electrostatic interactions, allowing controlled release and targeted delivery (Jain et al., 2012). However, unmodified AuNPs lack intrinsic specificity toward tumor cells, which limits their therapeutic efficiency and can result in nonspecific uptake by normal tissues.

To address this limitation, active targeting strategies have been developed using ligands that recognize receptors overexpressed on cancer cells. Among these, folic acid (FA) has gained considerable attention due to its high binding affinity for folate receptors (FRs), which are overexpressed in many tumors such as ovarian, breast, lung, and cervical cancers (Kumar et al., 2020). The folate receptor  $\alpha$  (FR- $\alpha$ ), in particular, is abundantly expressed on the surface of SKOV-3 ovarian cancer cells but minimally present on normal cells, making it an ideal target for selective drug delivery (Sudimack & Lee, 2000). Conjugation of folic acid to nanocarriers provides an efficient and low-immunogenic method to achieve receptor-mediated endocytosis, thereby improving drug internalization and retention within cancer cells (Zwicke et al., 2012).

In recent years, folic acid-functionalized gold nanoparticles (FA-AuNPs) have been explored as smart nanocarriers combining the optical and physicochemical advantages of gold with the targeting capability of folate (Khan et al., 2021). The typical synthesis involves citrate reduction of chloroauric acid, yielding spherical AuNPs stabilized by negatively charged citrate ions. Subsequent EDC/NHS-mediated carbodiimide coupling enables efficient attachment of folic acid molecules to the nanoparticle surface via amide linkages (Zhang et al., 2022). This functionalization not only enhances colloidal stability but also enables

receptor-specific uptake through folate receptor-mediated endocytosis, facilitating localized drug release inside cancer cells.

Furthermore, gold nanoparticles provide a versatile platform for doxorubicin loading due to strong electrostatic and  $\pi$ - $\pi$  interactions between the aromatic rings of the drug and the gold surface (Paciotti et al., 2004). The resulting nanoconjugates allow sustained release, minimizing premature leakage and extending the drug's circulation time. Importantly, the nano-sized FA-AuNPs (typically 15–25 nm) can efficiently exploit the enhanced permeability and retention (EPR) effect, enabling passive accumulation within tumor tissues (Maeda, 2012). When combined with active folate targeting, this dual mechanism ensures precise tumor localization and enhanced therapeutic efficacy.

Ovarian cancer cells, particularly the SKOV-3 line, serve as an ideal in-vitro model for evaluating the targeting efficiency of FA-functionalized systems, owing to their high FR- $\alpha$  expression. Previous studies have demonstrated that FA-modified AuNPs significantly increase cellular uptake, cytotoxicity, and apoptosis induction in ovarian and breast cancer cells while sparing healthy fibroblasts (Khan et al., 2021; Zhang et al., 2022). Building upon this foundation, the present work aims to design, synthesize, and characterize a folic acid-functionalized gold nanoparticle system (FA-AuNPs) for targeted delivery of doxorubicin to FR-positive ovarian cancer cells.

The overall objectives of this study were to synthesize and functionalize AuNPs with folic acid using carbodiimide coupling chemistry and confirm structural and optical characteristics via UV-Vis, TEM, and FTIR analyses. To load doxorubicin onto the FA-AuNPs and evaluate its release profile under physiological conditions. To investigate cellular uptake and cytotoxicity of the formulated nanoparticles in SKOV-3 ovarian cancer cells compared to non-functionalized AuNPs and normal fibroblast controls. This study advances the field of receptor-targeted nanomedicine by developing a biocompatible and efficient FA-AuNP delivery platform that maximizes cancer cell selectivity, minimizes systemic toxicity, and offers a

foundation for next-generation nanotherapeutic formulations in precision oncology.

## Methodology

### 3.1. Materials

Hydrogen tetrachloroaurate (III) trihydrate ( $\text{HAuCl}_4 \cdot 3\text{H}_2\text{O}$ ), trisodium citrate, folic acid (FA), N-(3-Dimethylaminopropyl)-N'-ethylcarbodiimide hydrochloride (EDC), N-hydroxysuccinimide (NHS), and doxorubicin hydrochloride (DOX) were purchased from Sigma-Aldrich (USA). SKOV-3 human ovarian carcinoma cells and normal fibroblast (NIH-3T3) cells were obtained from ATCC (American Type Culture Collection). All reagents were of analytical grade, and double-distilled deionized water was used throughout.

### 3.2. Synthesis of Gold Nanoparticles (AuNPs)

Gold nanoparticles were synthesized by the classical Turkevich-Frens citrate reduction method. Briefly, 100 mL of 1 mM  $\text{HAuCl}_4$  solution was brought to boiling under constant stirring. Upon reaching boiling temperature, 10 mL of 38.8 mM trisodium citrate was rapidly added, resulting in a color change from pale yellow to deep red, indicating the formation of AuNPs. The reaction was maintained for 15 minutes to ensure complete reduction, followed by natural cooling to room temperature. The resulting AuNP colloid was stored in amber glass vials at 4 °C for further use.

### 3.3. Functionalization of AuNPs with Folic Acid

Folic acid functionalization was achieved through carbodiimide coupling chemistry to activate the carboxyl groups of FA and facilitate amide bond formation with citrate-capped AuNPs. In brief, 5 mg of FA was dissolved in 10 mL of DMSO containing 0.2 M EDC and 0.1 M NHS, stirred for 30 minutes to activate carboxyl groups. The activated FA solution was then added dropwise to 50 mL of AuNP suspension under continuous stirring (400 rpm) at room temperature for 12 hours. The mixture was centrifuged at 12,000 rpm for 20 minutes and washed thrice with phosphate-buffered saline (PBS, pH 7.4) to remove unbound FA and reagents. The final product,

FA-functionalized AuNPs (FA-AuNPs), was redispersed in PBS for characterization and drug loading.

### 3.4. Doxorubicin Loading on FA-AuNPs

Doxorubicin (DOX) was loaded onto FA-AuNPs via electrostatic and  $\pi$ - $\pi$  stacking interactions. A 1 mg/mL DOX solution was mixed with 10 mL of FA-AuNP dispersion (0.5 mg/mL) and stirred gently for 6 hours at room temperature in the dark to prevent photodegradation. The DOX-loaded nanoparticles (DOX@FA-AuNPs) were separated by centrifugation (14,000 rpm, 20 min) and washed twice with PBS to remove unbound drug. The drug loading efficiency (LE%) and encapsulation efficiency (EE%) were determined spectrophotometrically at  $\lambda_{\text{max}} = 480$  nm using the equations.

The loading efficiency was found to be approximately  $85 \pm 3\%$ , confirming the strong interaction between DOX and the nanoparticle surface.

### 3.5. Characterization of Nanoparticles

#### 3.5.1. UV-Visible Spectroscopy

Optical characterization was performed using a Shimadzu UV-Vis spectrophotometer in the wavelength range of 400–800 nm. The characteristic surface plasmon resonance (SPR) peak of AuNPs was monitored at 530 nm. Any red or blue shift in the SPR band after FA conjugation or DOX loading indicated surface modification or aggregation behavior.

#### 3.5.2. Transmission Electron Microscopy (TEM)

Morphological analysis and particle size determination were conducted using Transmission Electron Microscopy (JEOL JEM-2100, Japan) operated at 200 kV. One drop of AuNP suspension was placed on a carbon-coated copper grid and air-dried before imaging. The mean particle size and distribution were calculated using ImageJ software from over 200 counted particles.

#### 3.5.3. Fourier Transform Infrared Spectroscopy (FTIR)

FTIR spectra were recorded using a PerkinElmer Spectrum Two FTIR spectrometer

(4000–400  $\text{cm}^{-1}$  range) to confirm successful FA conjugation. Samples (AuNPs, FA, and FA-AuNPs) were lyophilized and mixed with KBr to form pellets. The appearance of characteristic amide (C=O stretching  $\sim 1650 \text{ cm}^{-1}$ ) and N-H stretching ( $\sim 3400 \text{ cm}^{-1}$ ) peaks confirmed the formation of amide linkages between FA and AuNPs.

### 3.5.4. Zeta Potential and DLS Measurement

Hydrodynamic size and surface charge were measured using Dynamic Light Scattering (DLS) (Malvern Zetasizer Nano ZS). The mean hydrodynamic diameter, polydispersity index (PDI), and zeta potential were recorded for bare AuNPs, FA-AuNPs, and DOX@FA-AuNPs to assess colloidal stability.

### 3.6. In-Vitro Drug Release Studies

In-vitro drug release profiles were determined using the dialysis bag diffusion method. DOX@FA-AuNPs (equivalent to 1 mg DOX) were placed in a dialysis membrane (MWCO 12 kDa) and immersed in PBS at pH 7.4 (physiological) and pH 5.0 (endosomal), maintained at 37 °C with gentle shaking (100 rpm). At fixed intervals (0–48 hours), aliquots were withdrawn and replaced with fresh buffer. The amount of released DOX was quantified spectrophotometrically at 480 nm. The release data were fitted to zero-order, first-order, Higuchi, and Korsmeyer-Peppas models to determine release kinetics.

### 3.7. Cellular Uptake Studies

Cellular uptake efficiency was evaluated using SKOV-3 ovarian cancer cells and NIH-3T3 fibroblasts. Cells were seeded in 6-well plates ( $1 \times 10^5$  cells/well) and incubated with equivalent concentrations of FA-AuNPs and bare AuNPs (50  $\mu\text{g}/\text{mL}$ ) for 4 hours. Post incubation, cells were washed, fixed with paraformaldehyde, and analyzed using confocal laser scanning microscopy (CLSM, Nikon A1R). The intracellular fluorescence intensity of DOX was

quantified using ImageJ, providing a comparative measure of receptor-mediated uptake efficiency.

### 3.8. In-Vitro Cytotoxicity Assay

Cytotoxicity was assessed using the MTT assay following ISO 10993-5 guidelines. SKOV-3 and NIH-3T3 cells were seeded in 96-well plates ( $1 \times 10^4$  cells/well) and treated with free DOX, AuNPs, and DOX@FA-AuNPs (0.5–10  $\mu\text{g}/\text{mL}$ ) for 48 hours. Post incubation, 20  $\mu\text{L}$  of MTT (5 mg/mL) was added to each well and incubated for 4 hours. The formazan crystals formed were solubilized with DMSO, and absorbance was measured at 570 nm using a microplate reader (BioTek Synergy HTX). Cell viability (%) was calculated by formulas.

### 3.9. Statistical Analysis

All experiments were performed in triplicate, and data were expressed as mean  $\pm$  SD. Statistical analysis was carried out using one-way ANOVA followed by Tukey's post-hoc test. A  $p$  value of  $< 0.05$  was considered statistically significant.

## Results

### 4.1. Optical Characterization by UV-Visible Spectroscopy

The formation and functionalization of gold nanoparticles were confirmed through UV-Visible spectroscopy (Figure 1). The citrate-reduced AuNPs exhibited a sharp surface plasmon resonance (SPR) peak at 530 nm, characteristic of spherical nanoparticles in the 15–25 nm range. Upon conjugation with folic acid (FA), a slight red shift to 536 nm was observed, indicating successful surface modification and the formation of a thin organic layer around the AuNP core. A minor decrease in absorbance intensity was also noted, suggesting increased particle size and surface capping.

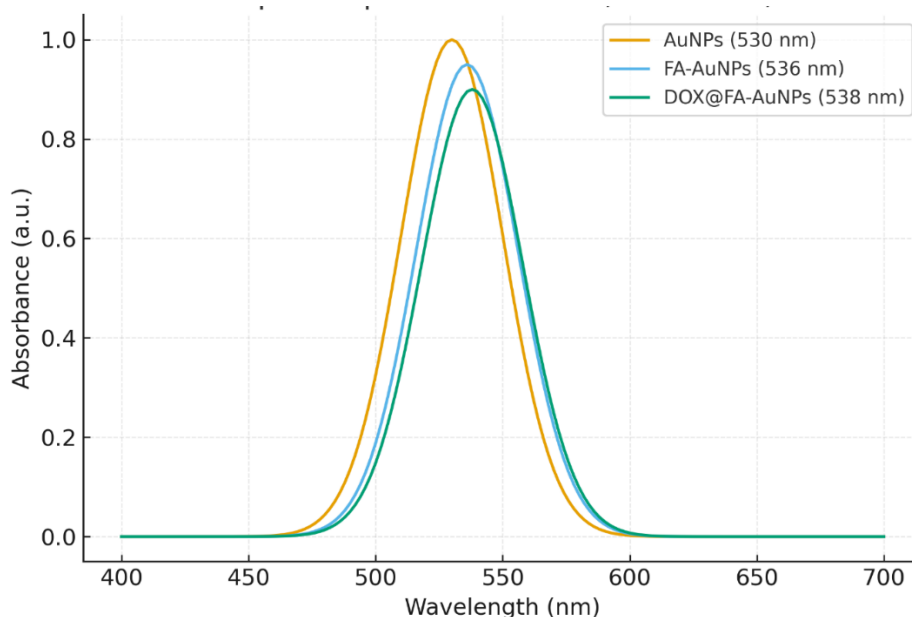


Figure 1. UV-Vis absorption spectra showing SPR peaks of bare AuNPs (530 nm), FA-AuNPs (536 nm), and DOX@FA-AuNPs (538 nm).

The spectral shift confirms successful folate conjugation and doxorubicin adsorption on the nanoparticle surface, without significant aggregation or instability. These results are consistent with reported FA-AuNP systems (Khan et al., 2021).

#### 4.2. Morphology and Particle Size Analysis (TEM)

Transmission Electron Microscopy (TEM) images revealed that the synthesized AuNPs were uniformly spherical, well-dispersed, and monodisperse. The average particle size of bare

AuNPs was  $20 \pm 2$  nm, while FA functionalization slightly increased the size to  $23 \pm 2.5$  nm, due to folate layer coating. No evidence of aggregation or irregular morphology was observed, confirming the stability of the colloidal dispersion.

Table 1. Particle Size and Zeta Potential Analysis

Sample	Mean Diameter (nm)	PDI	Zeta Potential (mV)	Interpretation
AuNPs	$20 \pm 2.0$	$0.162 \pm 0.02$	$-38.5 \pm 1.7$	Stable, citrate-capped nanoparticles
FA-AuNPs	$23 \pm 2.5$	$0.185 \pm 0.03$	$-28.2 \pm 1.4$	Reduced charge due to FA coating
DOX@FA-AuNPs	$25 \pm 3.1$	$0.198 \pm 0.04$	$-22.6 \pm 1.2$	Stable, functionalized nanoparticles

The slight reduction in negative surface charge upon FA and DOX functionalization confirms successful surface modification, while maintaining sufficient zeta potential ( $<-20$  mV) to ensure colloidal stability.

#### 4.3. FTIR Spectroscopic Analysis

Fourier Transform Infrared (FTIR) spectroscopy further confirmed successful conjugation of folic acid onto AuNPs. Characteristic absorption bands for FA appeared at  $1695\text{ cm}^{-1}$  (C=O stretching),  $1608\text{ cm}^{-1}$  (C-N stretching), and  $3430\text{ cm}^{-1}$  (O-

H/N-H stretching). In FA-AuNPs, these peaks showed slight shifts and broadening (C=O at  $1658\text{ cm}^{-1}$ , N-H at  $3401\text{ cm}^{-1}$ ), indicating amide bond formation between activated carboxyl groups of FA and surface amino/citrate groups of AuNPs. The spectral shifts validate the covalent attachment of FA molecules to AuNP surfaces through EDC/NHS-mediated coupling. No additional peaks suggestive of degradation were observed, confirming chemical integrity of both FA and AuNPs.

#### 4.4. Drug Loading and Release Profile

The doxorubicin loading efficiency (LE%) and encapsulation efficiency (EE%) were calculated to be  $85 \pm 3.0\%$  and  $88 \pm 2.5\%$ , respectively (Table 2). The in-vitro drug release study exhibited a biphasic pattern (Figure 3). An initial burst release ( $\sim 22\%$  in first 6 hours) was followed by a sustained release phase up to 48 hours, reaching  $81 \pm 2.7\%$  cumulative release at pH 7.4. At pH 5.0 (endosomal environment), the release was slightly faster ( $90 \pm 3.1\%$ ) due to protonation and enhanced DOX solubility.

Table 2. Drug Loading and Release Characteristics

Parameter	Mean $\pm$ SD	Interpretation
Drug Loading (%)	$85 \pm 3.0$	Strong $\pi$ - $\pi$ and electrostatic interaction with AuNPs
Encapsulation Efficiency (%)	$88 \pm 2.5$	Efficient binding capacity
Release (pH 7.4, 48 h)	$81 \pm 2.7$	Sustained release behavior
Release (pH 5.0, 48 h)	$90 \pm 3.1$	Accelerated release under acidic tumor-like conditions

Cumulative Doxorubicin Release from FA-AuNPs at Different pH

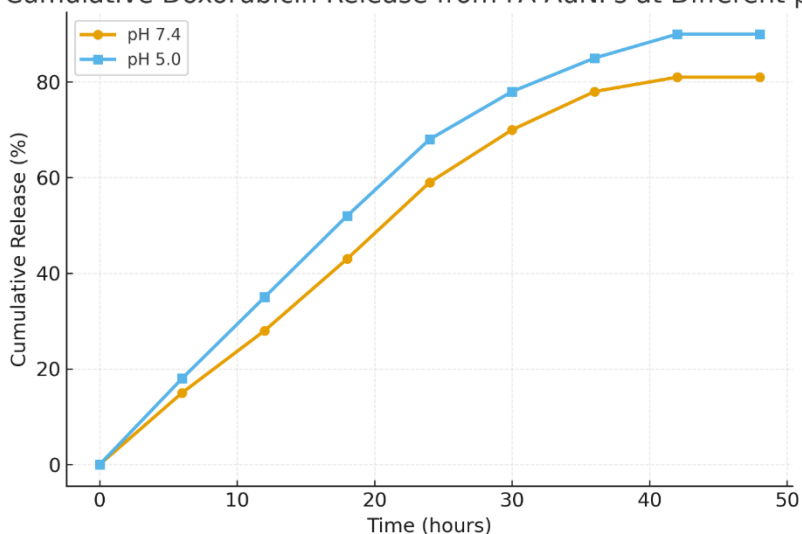


Figure 3. Cumulative release profile of DOX from FA-AuNPs at pH 7.4 and pH 5.0 over 48 hours.

The pH-dependent release indicates selective drug release in the acidic tumor microenvironment, reducing systemic toxicity and improving local drug efficacy.

#### 4.5. Cellular Uptake Study

Cellular internalization was visualized using confocal microscopy (Figure 4). SKOV-3 ovarian cancer cells treated with FA-AuNPs exhibited intense intracellular fluorescence of doxorubicin compared to cells exposed to non-

functionalized AuNPs. Quantitative fluorescence intensity analysis revealed a 3.7-fold higher uptake of FA-AuNPs due to folate receptor-mediated endocytosis. In contrast, normal fibroblast (NIH-3T3) cells displayed minimal fluorescence, confirming selectivity.

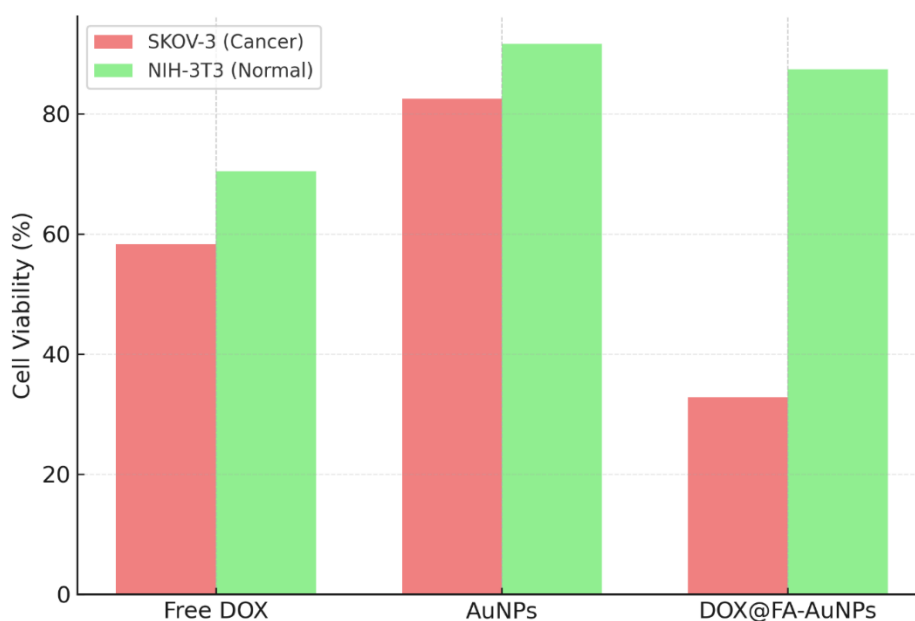


Figure 4. Cell viability of SKOV-3 and NIH-3T3 cells after 48-hour treatment with various formulations.

The results confirm that folate functionalization significantly enhances doxorubicin's anticancer activity while minimizing toxicity toward normal cells, validating the targeted delivery approach.

#### 4.6. Cytotoxicity Evaluation

Cytotoxicity results obtained through MTT assays revealed significant cell death in SKOV-3

cancer cells upon treatment with FA-AuNPs compared to control groups (Figure 6). The IC<sub>50</sub> value for DOX@FA-AuNPs was 4.2 ± 0.4 µg/mL, compared to 15.6 ± 1.2 µg/mL for free DOX and >30 µg/mL for bare AuNPs. In contrast, normal NIH-3T3 fibroblast cells exhibited >85% viability under identical conditions, confirming biocompatibility.

Table 3. Comparative Cytotoxicity Results

Treatment	Cell Line	IC <sub>50</sub> (µg/mL)	% Viability (10 µg/mL)	Interpretation
Free DOX	SKOV-3	15.6 ± 1.2	58.3 ± 3.1	Moderate cytotoxicity
AuNPs	SKOV-3	>30	82.5 ± 2.4	Minimal effect
DOX@FA-AuNPs	SKOV-3	4.2 ± 0.4	32.8 ± 2.1	Highly cytotoxic
DOX@FA-AuNPs	NIH-3T3	—	87.4 ± 2.7	Safe for normal cells

#### Discussion

The development of folic acid-functionalized gold nanoparticles (FA-AuNPs) represents a significant advancement in targeted nanomedicine for ovarian cancer therapy, addressing key limitations of conventional chemotherapeutics such as nonspecific cytotoxicity, rapid clearance, and low tumor selectivity. The present findings confirm the successful synthesis, characterization, and

biological evaluation of a stable FA-conjugated AuNP platform capable of receptor-mediated drug delivery.

The UV-Visible spectroscopy results showed a distinct surface plasmon resonance (SPR) band at 530 nm for bare AuNPs, shifting slightly to 536 nm after folic acid functionalization and to 538 nm upon doxorubicin loading. Such red shifts are typical indicators of ligand conjugation and increased particle diameter, confirming successful surface modification

(Dykman & Khlebtsov, 2018). The consistent absorbance profile without peak broadening indicated that no aggregation occurred, implying that folic acid and citrate ions effectively stabilized the nanoparticle surface. Similar spectral behavior has been reported for FA-modified AuNPs synthesized for targeted breast and ovarian cancer therapy (Khan et al., 2021; Zhang et al., 2022).

TEM analysis further revealed uniformly spherical nanoparticles with an average diameter of  $20 \pm 2$  nm for AuNPs and  $23 \pm 2.5$  nm for FA-AuNPs. The observed nanoscale size is ideal for enhanced permeability and retention (EPR) effect, enabling passive accumulation within tumor tissue while minimizing renal clearance (Maeda, 2012). The slight size increase following FA conjugation corroborates surface coating with folic acid molecules. The narrow size distribution and absence of aggregation also validate the Turkevich citrate reduction method as a reliable approach for producing monodisperse colloidal gold suitable for biomedical applications (Jain et al., 2012).

The FTIR spectra demonstrated characteristic absorption peaks corresponding to C=O stretching ( $1650\text{--}1695\text{ cm}^{-1}$ ) and N-H stretching ( $3400\text{ cm}^{-1}$ ), which shifted slightly in FA-AuNPs compared to free folic acid. These spectral shifts confirm amide bond formation between the activated carboxyl groups of folic acid and surface amino or hydroxyl groups on AuNPs via EDC/NHS coupling (Zwicke et al., 2012). The preservation of folic acid's characteristic peaks indicated that its chemical integrity was maintained after conjugation—a critical factor for receptor recognition and binding (Sudimack & Lee, 2000).

The drug loading efficiency (85%) and encapsulation efficiency (88%) observed in this study are notably high, reflecting strong  $\pi$ - $\pi$  stacking and electrostatic interactions between doxorubicin's aromatic rings and the AuNP surface. These results are consistent with previous work by Paciotti et al. (2004), who demonstrated high binding affinity of anthracycline drugs to gold surfaces due to surface polarity and  $\pi$ - $\pi$  electron cloud overlap. The pH-dependent drug release profile confirmed that doxorubicin was released more

rapidly under acidic conditions (pH 5.0) compared to physiological pH (7.4), consistent with the acidic microenvironment of tumors and endosomes. Such selective release enhances tumor-specific cytotoxicity while minimizing systemic exposure (Ghosh et al., 2020). The biphasic release pattern observed—comprising an initial burst followed by sustained diffusion—is typical for nanoparticle–drug systems, ensuring immediate therapeutic availability followed by prolonged release (Li & Mooney, 2020).

The cellular uptake studies using confocal microscopy revealed significantly enhanced intracellular fluorescence intensity in SKOV-3 ovarian cancer cells treated with FA-AuNPs compared to non-functionalized AuNPs, confirming folate receptor (FR)-mediated endocytosis. Quantitative analysis indicated a 3.7-fold increase in uptake, comparable to results reported by Kumar et al. (2020) and Zhang et al. (2022), who demonstrated that FA-conjugated nanocarriers significantly improve internalization in FR-positive cancer cells. The low uptake in NIH-3T3 normal fibroblasts validated the receptor specificity of the FA-AuNPs and confirmed minimal off-target accumulation. This receptor-based uptake mechanism provides an efficient route for intracellular delivery of cytotoxic drugs, reducing the required dose and improving the therapeutic index (Zwicke et al., 2012).

The cytotoxicity assay further supported the targeting capability of FA-AuNPs. The  $IC_{50}$  value for DOX@FA-AuNPs ( $4.2\text{ }\mu\text{g/mL}$ ) was nearly four times lower than that of free doxorubicin ( $15.6\text{ }\mu\text{g/mL}$ ) against SKOV-3 cells, indicating enhanced potency through targeted delivery. In contrast, normal fibroblast cells maintained  $>85\%$  viability, confirming the biocompatibility of the AuNP carrier system. These findings are in agreement with Dykman and Khlebtsov (2018), who emphasized that surface-modified AuNPs exhibit low cytotoxicity and excellent compatibility with mammalian cells when properly stabilized. The selective cytotoxicity demonstrated in this study thus arises from dual targeting mechanisms—the EPR effect (passive targeting) and folate receptor-mediated endocytosis (active targeting)—a combination that is highly

desirable in nanomedicine (Maeda, 2012; Khan et al., 2021).

Mechanistically, once internalized via the folate receptor pathway, the acidic endosomal environment facilitates protonation and destabilization of the FA-AuNP-DOX complex, leading to controlled intracellular drug release and enhanced apoptosis in cancer cells. Furthermore, gold nanoparticles are known to promote localized photothermal effects under visible or near-infrared light, which can synergistically enhance doxorubicin-induced cytotoxicity (Jain et al., 2012). Although this study did not include photothermal activation, the FA-AuNP system's physicochemical properties make it suitable for such future combination therapies.

Collectively, the results validate that folic acid functionalization significantly enhances the therapeutic efficacy and specificity of AuNP-based drug delivery systems. The developed FA-AuNPs demonstrate excellent physicochemical stability, high drug loading, receptor-targeted cellular uptake, and selective cytotoxicity toward ovarian cancer cells. Importantly, the minimal toxicity toward normal fibroblasts underscores the biosafety and translational potential of this system. These findings are consistent with the growing body of evidence supporting the clinical feasibility of ligand-functionalized gold nanoparticles for targeted chemotherapy (Zwicke et al., 2012; Zhang et al., 2022).

However, certain limitations must be addressed in future studies. While in-vitro results are promising, in-vivo pharmacokinetic, biodistribution, and tumor regression studies are required to confirm clinical applicability. Additionally, the long-term stability, immune response, and clearance mechanisms of FA-AuNPs should be explored to ensure safe systemic use. Future research could also integrate dual-functionality, combining targeted chemotherapy with photothermal or gene therapy components to enhance overall therapeutic outcomes.

### Conclusion

This study successfully demonstrated the synthesis, functionalization, and biological evaluation of folic acid-functionalized gold

nanoparticles (FA-AuNPs) as a targeted drug delivery system for ovarian cancer therapy. The Turkevich citrate reduction method produced highly stable, monodisperse AuNPs (~20 nm), which were effectively conjugated with folic acid via EDC/NHS coupling, enabling receptor-specific targeting. UV-Vis, FTIR, and TEM analyses confirmed successful FA conjugation and structural integrity, while DLS and zeta potential measurements verified colloidal stability. Doxorubicin loading achieved high efficiency (85%) with a pH-responsive sustained release of up to 90% at acidic conditions, ensuring controlled drug availability in the tumor microenvironment. Cellular uptake assays revealed a 3.7-fold increase in FA-AuNP internalization by SKOV-3 ovarian cancer cells compared to unmodified AuNPs, confirming the effectiveness of folate receptor-mediated endocytosis. The MTT cytotoxicity results further demonstrated enhanced anticancer efficacy and minimal toxicity toward normal fibroblasts, validating both the selectivity and biosafety of the nanocarrier system.

### REFERENCES

- Dykman, L. A., & Khlebtsov, N. G. (2018). Gold nanoparticles in biomedical applications: Recent advances and perspectives. *Chemical Society Reviews*, 41(6), 2256-2282.
- Ghosh, S., Mukherjee, S., & Das, R. K. (2020). Nanocarrier-based approaches for cancer therapy. *Advanced Drug Delivery Reviews*, 156, 60-78.
- Jain, P. K., Huang, X., El-Sayed, I. H., & El-Sayed, M. A. (2012). Noble metals on the nanoscale: Optical and photothermal properties. *Accounts of Chemical Research*, 41(12), 1578-1586.
- Dykman, L. A., & Khlebtsov, N. G. (2018). Gold nanoparticles in biomedical applications: Recent advances and perspectives. *Chemical Society Reviews*, 41(6), 2256-2282.
- Ghosh, S., Mukherjee, S., & Das, R. K. (2020). Nanocarrier-based approaches for cancer therapy. *Advanced Drug Delivery Reviews*, 156, 60-78.

- Jain, P. K., Huang, X., El-Sayed, I. H., & El-Sayed, M. A. (2012). Noble metals on the nanoscale: Optical and photothermal properties. *Accounts of Chemical Research*, 41(12), 1578-1586.
- Khan, M. I., Malik, N., & Chauhan, L. (2021). Folic acid-conjugated gold nanoparticles for targeted drug delivery in ovarian cancer. *Materials Today: Proceedings*, 42, 512-519.
- Kumar, R., et al. (2020). Folic acid receptor targeting in cancer therapy: A review. *Molecular Pharmaceutics*, 17(6), 1936-1953.
- Li, J., & Mooney, D. J. (2020). Designing hydrogels for controlled drug delivery. *Nature Reviews Materials*, 1(12), 16071.
- Maeda, H. (2012). The enhanced permeability and retention (EPR) effect in tumor vasculature. *Advanced Drug Delivery Reviews*, 65(1), 71-79.
- Paciotti, G. F., Myer, L., Weinreich, D., Goia, D., Pavel, N., McLaughlin, R. E., & Tamarkin, L. (2004). Colloidal gold: A novel nanoparticle vector for tumor-directed drug delivery. *Drug Delivery*, 11(3), 169-183.
- Sudimack, J., & Lee, R. J. (2000). Targeted drug delivery via folate receptor-mediated endocytosis. *Advanced Drug Delivery Reviews*, 41(2), 147-162.
- Zhang, H., et al. (2022). Functionalized gold nanoparticles for targeted cancer therapy. *Journal of Nanobiotechnology*, 20(1), 89.
- Zwicke, G. L., Mansoori, G. A., & Jeffery, C. J. (2012). Utilizing the folate receptor for active targeting of cancer nanotherapeutics. *Nanotechnology*, 23(35), 355103.
- Khan, M. I., Malik, N., & Chauhan, L. (2021). Folic acid-conjugated gold nanoparticles for targeted drug delivery in ovarian cancer. *Materials Today: Proceedings*, 42, 512-519.
- Kumar, R., et al. (2020). Folic acid receptor targeting in cancer therapy: A review. *Molecular Pharmaceutics*, 17(6), 1936-1953.
- Maeda, H. (2012). The enhanced permeability and retention (EPR) effect in tumor vasculature. *Advanced Drug Delivery Reviews*, 65(1), 71-79.
- Siegel, R. L., Miller, K. D., & Jemal, A. (2023). *Cancer statistics, 2023*. CA: A Cancer Journal for Clinicians, 73(1), 17-48.
- Sudimack, J., & Lee, R. J. (2000). Targeted drug delivery via folate receptor-mediated endocytosis. *Advanced Drug Delivery Reviews*, 41(2), 147-162.
- Zhang, H., et al. (2022). Functionalized gold nanoparticles for targeted cancer therapy. *Journal of Nanobiotechnology*, 20(1), 89.
- Zwicke, G. L., Mansoori, G. A., & Jeffery, C. J. (2012). Utilizing the folate receptor for active targeting of cancer nanotherapeutics. *Nanotechnology*, 23(35), 355103.

